Preprint, 11th IFAC Symposium on Dynamics and Control of Process Systems,
including Biosystems
June 6-8, 2016. NTNU, Trondheim, Norway

Model Development for Phosphate Recovery from Acidic Wastewater

Mihaela Sbarciog * **Alain Vande Wouwer** *

* *Automatic Control Laboratory, University of Mons, Boulevard Dolez 31, B-7000 Mons, Belgium (e-mail: {MihaelaIuliana.Sbarciog, Alain.VandeWouwer}@umons.ac.be).*

Abstract: This paper presents an original model for calcium phosphate crystallization from acidic wastewater. The model is developed using classical principles of chemistry and population balance modeling. The aim is to further use the model for analysis, control and optimization of the crystallization process for phosphate recovery. The proposed model consists of one population balance equation coupled with four mass balance equations and a set of algebraic equations, which can be easily integrated with Matlab and MatMOL toolbox. The model is validated against PHREEQC, a software for speciation and geochemical calculations.

Keywords: Modelling, chemical industry, partial differential equations, simulators

1. INTRODUCTION

The disposal of industrial wastewater containing sometimes mixtures of acids poses a real challenge as it involves water loses, valuable chemicals loses and most importantly it leads to the environment damage once this wastewater reaches the ground water. Therefore, before being disposed the industrial acidic wastewater must undergo some purification or treatment for removing the impurities and reducing the acid content to the admissible limits imposed by the regulations on the water quality. On the other hand, the natural resources of some chemicals such as phosphate and fluoride have decreased drastically due to their extensive use as raw materials. Hence, their recovery from industrial wastewater is important in view of the potential reuse in industry, leading thus to a sustainable development.

Several techniques are available for the recovery of minerals from wastewater, among which the precipitation and crystallization are the most used ones due to their simplicity. These processes involve the addition of salts (among which the calcium salts are the less expensive ones) to the acidic wastewater. The disadvantage of using the precipitation technique lies in the fact that usually small particles that are too fine to settle are produced. Thus sludge with high water content and low quality is generated. In the crystallization process however, the water content of the sludge is greatly decreased as the retention time is prolonged. Hence, the crystals grow to a significant size, allowing an easy separation and reuse (Jiang et al., 2014). Although there is a difference between precipitation and crystallization, these terms are mostly used as synonyms, which will be also the case here.

The study of precipitation and crystallization processes is an active field of research, which has received a lot of attention especially from the perspective of the numerous experimental investigations and the purely chemical theoretical works performed so far. Phosphate precipitation studies are widely encountered, probably due to the many forms of phosphates under which precipitation with calcium salts can occur (dicalcium phosphate dehydrate - DCPD, octacalcium phosphate - OCP, amorphous calcium phosphate - ACP, tricalcium phosphate - TCP and hydroxyapatite - HAP), but also due to its precipitation with magnesium salts, which is usually used to recover nitrogen and phosphorus from wastewater as struvite.

Among the studies related to the precipitation of calcium phosphate, a great deal of work has been performed by Nancollas and his co-workers (Nancollas and Gardner, 1974; Barone et al., 1976; Barone and Nancollas, 1977). Nancollas and Koutsoukos (1980) studied the precipitation of various forms of calcium phosphates using a constant composition method, which allowed the assessment of the influence of pH, supersaturation, seed type and concentration and traces of added substances. Such a study has been performed also for the precipitation of hydroxyapatite (HAP) (Koutsoukos et al., 1980). Additionally, a model for the rate of crystallization in the form of a differential equation has been proposed.

Since then, many works on the precipitation and crystallization of calcium phosphate have been published. For example, Boistelle and Astier (1988) have presented a survey on the nucleation, growth, phase transition and ripening intended to illustrate the fact that crystallization is a sequence of events that occur consecutively and are interconnected. This has been later on applied to the case of the calcium phosphates by Boistelle and Lopez-Valero (1990). Fernandez et al. (1999a,b) have reviewed the solution chemistry of calcium phosphates to highlight the way in which the thermodynamics of these systems has influenced the development of the various calcium phosphate cement formulations and presented also a literature review concerning the precipitate formation during the setting reactions in the system $Ca\text{-}P\text{-}H_2O$. Song et al. (2002) have investigated the effects of the solution conditions on the phosphate precipitation by using specialized software for computing the speciation and supersaturation. Hosni et al. (2008) have studied the feasibility of phosphate removal from synthetic wastewater by precipitation with calcium hydroxide addition in order to determine optimal operating conditions in terms of optimal Ca/P molar ratio and time of the precipitation. Wang and Nan-

collas (2008) have reviewed some important parameters related to crystal nucleation and growth/dissolution including the supersaturation/undersaturation, pH, ionic strength and the ratio of calcium to phosphate activities. Castro et al. (2012) have studied different experimental conditions by varying the Ca/P molar ratio and have characterized the precipitation process in function of pH and calcium concentration. Subsequently (Castro et al., 2013), they have investigated an ultrasonic tubular microreactor for the continuous-flow precipitation of hydroxyapatite, concluding that the obtained particles show improved characteristics compared to the commercial powder.

Even without a more extensive literature review, one may notice that, in spite of the wide use of precipitation and crystallization, the majority of the available studies still deal with understanding the key thermodynamics and the kinetics of these processes and characterize the crystallizer performance in terms of the yield rather than the product quality, which is described by particle size distribution, morphology, polymorphism, uptake of solvent or impurities in the crystal lattice (Vedantam and Ranade, 2013). Studies involving both, the thermodynamics and the crystal size distribution, are scarce. Among them, of noticeable importance is the one presented by Oliveira et al. (2007) who have built a dynamic model for the transformation of hydroxyapatite into dicalcium phosphate dihydrate (brushite) and the growth of brushite, and have identified the model parameters from experimental data consisting of on-line measurements of the calcium concentration in solution and off-line measurements of the particle size distribution. Hanhoun et al. (2013) have coupled the thermodynamic model with the crystal size distribution modeling and have identified the kinetic parameters for the precipitation of struvite in a batch reactor. Galbraith and Schneider (2014) have proposed also a model to simulate the precipitation of struvite in a mixed suspension mixed product removal reactor by including nucleation, growth and aggregation phenomena, and using kinetic parameters from literature.

In this paper we propose a dynamic model for calcium phosphate crystallization as hydroxyapatite (the most stable form of calcium phosphate), which precipitates from solutions at higher pH values without an intermediate phase. The model takes into account the system thermodynamics, the transfer between the liquid and solid phases and describes the evolution of the particle size distribution. It is built with the aim of being further used for the analysis, control and optimization of the calcium phosphate precipitation process, thus representing a good compromise between accuracy and simplicity. The model consists of four mass balances, one population balance equation and a set of algebraic equations, which can be easily solved with Matlab and MatMOL toolbox (Vande Wouwer et al., 2005). Simulation results are presented to show the prediction capability of the model. A comparison of the model thermodynamics with the results provided by PHREEQC (Parkhurst and Appelo, 2013), a well-known software that performs a wide variety of aqueous geochemical calculations, is included to illustrate the model accuracy.

The paper is organized as follows: Section 2 introduces the basic definitions and presents the main steps in the model development; Section 3 briefly describes the process to be modelled, while Section 4 details the model development. Simulation results are presented in Section 5 and conclusions and perspectives are stated in Section 6.

2. MODEL RATIONALES

Chemical precipitation (crystallization) is a complex nonlinear process, influenced by many factors (e.g. many species, temperature, pH, etc.) and particularly difficult due to the presence of the two phases: liquid and solid. Hence, an accurate model must characterize each of the two phases, as well as the transition between the phases. Thus, the model developed in this work is composed of four interconnected elements (Galbraith and Schneider, 2014), which describe together the dynamics of the precipitation process:

- Solution thermodynamics - establishes the conditions for precipitation;
- Kinetics - describes the nucleation and crystals growth rates;
- Population balance - describes the evolution of the particle size distribution;
- Mass balance - evaluates how much solute has been transferred from the liquid to the solid phase.

2.1 Solution thermodynamics

In any crystallization system, the solution thermodynamics characterizes the conditions for the occurrence of the precipitation (Mullin, 2001). A key element for the precipitation to occur is the condition of solution supersaturation: a solution is supersaturated when the solute concentration exceeds its equilibrium concentration. However, in the case of multi-ionic systems, like the one we deal with in this study, the supersaturation ratio is defined in terms of the ion activity product (IAP) as

$$S = \left(\frac{IAP}{K_{sp}}\right)^{\frac{1}{\nu}} \tag{1}$$

where K_{sp} is the solubility product (i.e. the value of the IAP at equilibrium) and ν is the number of ions in a formula unit of the salt. The calculation of the ion activity product (IAP) requires the knowledge of the chemical speciation of the ions in solution. Thus, it is first necessary to identify all the possible single species, ion pairs and solid-liquid equilibria in the system. Also the relevant thermodynamic association/dissociation constants must be known.

In supersaturated solutions the chemical interaction between ions becomes important and cannot be neglected. In this situation, a species c_i is characterized by its activity, which is related to the species concentration by means of an activity coefficient:

$$\{c_i\} = \gamma_i \cdot (c_i) \tag{2}$$

where $\{c_i\}$ denotes the activity of c_i, (c_i) denotes the concentration of c_i and γ_i denotes the activity coefficient. The activity coefficients can be calculated using some variant of the Debye-Hückel equation (Mullin, 2001). Here we use the Davies approximation:

$$-\log_{10}\gamma_i = AZ_i^2\left(\frac{\sqrt{I}}{1+\sqrt{I}} - 0.3I\right) \tag{3}$$

with the ionic strength I (a measure of the concentration of all ions in solution) given by:

$$I = \frac{1}{2}\sum (c_i)\, Z_i^2 \tag{4}$$

In (3), (4), Z_i is the valency of species c_i and A is the Debye-Hückel constant, which equals 0.509 at $25°C$.

Another key variable in the precipitation process is the solution pH, since many thermodynamic equilibria contain hydrogen ions. The pH is defined as

$$pH = -\log_{10}\left\{H^+\right\} \tag{5}$$

where $\{H^+\}$ denotes the activity of the hydrogen ions. It can be either specified or determined from a charge balance equation:

$$\sum (c_i)\, Z_i = 0 \tag{6}$$

2.2 Kinetics

The kinetics of a crystallization process refer to the nucleation and crystal growth, which require the change of free energy (Jones, 2002). Both nucleation and growth of crystals depend on the degree of supersaturation, but usually to different orders.

Nucleation is the first formation of the solid phase. It occurs due to clustering and aggregation of molecules or ions in supersaturated solutions to a size that such entities become viable. Primary nucleation is the "classical" form of nucleation, which occurs mainly at high levels of supersaturation. Gibbs considered the change of free energy during homogeneous nucleation, which leads to the classical nucleation theory and to the Gibbs-Thompson relationship (Mullin, 2001) for homogeneous nucleation:

$$r_N = A \exp\left(-\frac{B}{(\ln S)^2}\right) \tag{7}$$

where r_N represents the number of nuclei formed per unit time per unit volume; A and B are parameters; S is the supersaturation ratio.

Crystal growth is a diffusion and integration process, modified by the effect of the solid surfaces on which it occurs (Jones, 2002). The particle growth may be expressed as a rate of linear increase of characteristic dimension (i.e. velocity), $G = \frac{dL}{dt}$, where L is the characteristic dimension that is increasing.

Crystal growth may occur by a variety of mechanisms for which several theoretical models have been proposed as reviewed in (Söhnel and Garside, 1992; Mullin, 2001). However, these can be hardly used in practice as they depend on variables that cannot be measured or determined. Therefore, a simpler power law expression depending on the supersaturation is generally adopted, $G = k_g\,(S^r)^g$, where $S^r = S - 1$; k_g and g are kinetic parameters, estimated from experimental data and they respectively represent the crystal growth rate coefficient and the rate order.

3. PROCESS DESCRIPTION

The process to be modeled takes place in a crystallizer (Figure 1). The acidic wastewater, modeled here as a mix of orthophosphoric acid and hydrochloric acid, enters the reactor through the inlet flow q_{in_2}. Dissolved calcium hydroxide is added to the reactor with the inlet flow q_{in_1} to trigger and maintain the precipitation of calcium phosphate under the form of hydroxyapatite (HAP). As the goal is to obtain crystals of relatively large size, the crystallizer can be employed in semi-batch mode ($q_{out} = 0$, i.e., no component leaves the reactor before the end of the operation) or in continuous mode ($q_{out} = q_{in_1} + q_{in_2}$, i.e., mixed suspension, mixed product removal crystallizer). The process must be operated in such a way that a high amount of phosphorus is removed and recovered through HAP crystals of significant size.

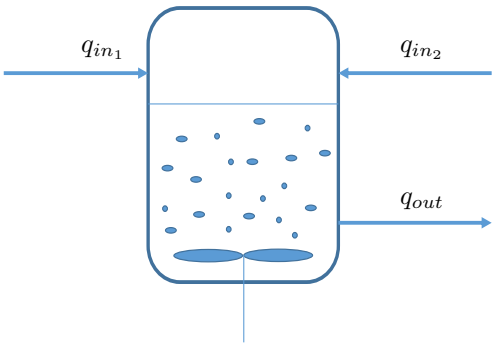

Fig. 1. Schematic representation of the crystallizer

We assume the presence of the following chemical species inside the reactor: H_3PO_4, $H_2PO_4^-$, HPO_4^{2-}, PO_4^{3-}, $CaPO_4^-$, $CaHPO_4$, $CaH_2PO_4^+$, $CaOH^+$, H^+, OH^-, Cl^-, and the occurrence of the following association/dissociation reactions, which are the most encountered ones in the system $Ca - P - H_2O$ (Oliveira et al., 2007):

$$H_3PO_4 \rightleftharpoons H_2PO_4^- + H^+ \tag{8}$$
$$H_2PO_4^- \rightleftharpoons HPO_4^{2-} + H^+ \tag{9}$$
$$HPO_4^{2-} \rightleftharpoons PO_4^{3-} + H^+ \tag{10}$$
$$CaPO_4^- \rightleftharpoons Ca^{2+} + PO_4^{3-} \tag{11}$$
$$CaHPO_4 \rightleftharpoons Ca^{2+} + HPO_4^{2-} \tag{12}$$
$$CaH_2PO_4^+ \rightleftharpoons Ca^{2+} + H_2PO_4^- \tag{13}$$
$$CaOH^+ \rightleftharpoons Ca^{2+} + OH^- \tag{14}$$
$$H_2O \rightleftharpoons H^+ + OH^- \tag{15}$$

The hydroxyapatite complex precipitates from the liquid phase with a rate r_s according to the chemical reaction:

$$5Ca^{2+} + 3PO_4^{3-} + OH^- \rightarrow Ca_5\,(PO_4)_3\,OH \tag{16}$$

4. MODEL DEVELOPMENT

4.1 Liquid phase

In the liquid phase we assume that the reactor is perfectly mixed and no changes in the volume occur due to the chemical reactions. Then the dynamics of the process are described by a set of differential equations, which express the changes in the reactor volume due to the influent flows and in the concentrations of the species due to the dilution and chemical reactions:

$$\frac{dV}{dt} = q_{in_1} + q_{in_2} - q_{out} \tag{17}$$

$$\frac{d(Ca^{2+})}{dt} = \frac{q_{in_1}}{V}(Ca_{in}^{2+}) - \frac{q_{in_1} + q_{in_2}}{V}(Ca^{2+}) - r_4 - r_5 - r_6 - r_7 - 5r_s \tag{18}$$

$$\frac{d(CaPO_4^-)}{dt} = \frac{q_{in_1}}{V}(CaPO_{4in}^-) - \frac{q_{in_1} + q_{in_2}}{V}(CaPO_4^-) + r_4 \tag{19}$$

$$\frac{d(CaHPO_4)}{dt} = \frac{q_{in_1}}{V}(CaHPO_{4in}) - \frac{q_{in_1} + q_{in_2}}{V}(CaHPO_4) + r_5 \tag{20}$$

$$\frac{d(CaH_2PO_4^+)}{dt} = \frac{q_{in_1}}{V}(CaH_2PO_{4in}^+) - \frac{q_{in_1}+q_{in_2}}{V}(CaH_2PO_4^+) + r_6 \quad (21)$$

$$\frac{d(CaOH^+)}{dt} = \frac{q_{in_1}}{V}(CaOH_{in}^+) - \frac{q_{in_1}+q_{in_2}}{V}(CaOH^+) + r_7 \quad (22)$$

$$\frac{d(H_3PO_4)}{dt} = \frac{q_{in_2}}{V}(H_3PO_{4in}) - \frac{q_{in_1}+q_{in_2}}{V}(H_3PO_4) + r_1 \quad (23)$$

$$\frac{d(H_2PO_4^-)}{dt} = \frac{q_{in_2}}{V}(H_2PO_{4in}^-) - \frac{q_{in_1}+q_{in_2}}{V}(H_2PO_4^-) + r_2 - r_1 - r_6 \quad (24)$$

$$\frac{d(HPO_4^{2-})}{dt} = \frac{q_{in_2}}{V}(HPO_{4in}^{2-}) - \frac{q_{in_1}+q_{in_2}}{V}(HPO_4^{2-}) + r_3 - r_2 - r_5 \quad (25)$$

$$\frac{d(PO_4^{3-})}{dt} = \frac{q_{in_2}}{V}(PO_{4in}^{3-}) - \frac{q_{in_1}+q_{in_2}}{V}(PO_4^{3-}) - r_3 - r_4 - 3r_s \quad (26)$$

$$\frac{d(OH^-)}{dt} = \frac{q_{in_1}}{V}(OH_{in_1}^-) + \frac{q_{in_2}}{V}(OH_{in_2}^-) - \frac{q_{in_1}+q_{in_2}}{V}(OH^-) - r_7 - r_s \quad (27)$$

$$\frac{d(Cl^-)}{dt} = \frac{q_{in_2}}{V}(Cl_{in}^-) - \frac{q_{in_1}+q_{in_2}}{V}(Cl^-) \quad (28)$$

In (17)-(28), q_{in_1} and q_{in_2} represent the influent flows, respectively containing calcium and phosphate ions, while q_{out} is the effluent flow; V is the reactor volume; $(.)$ represents the species concentration; r_i, with $i = 1 \dots 7$, are respectively the rates of the chemical reactions (8)-(14), while r_s represents the rate of the precipitation reaction (16).

Generally, the chemical reactions (8)-(14) are very fast, therefore chemical equilibrium is assumed in the liquid phase. The relationships between the species at the chemical equilibrium and the corresponding equilibrium constants are given in Table 1, where $\{.\}$ denotes the species activity.

Hence, the rates r_i, $i = 1 \dots 7$ are no longer defined. However, the model (17)-(28) can be recast by considering the total atoms of a certain component present in the system. Let us define the total calcium, total phosphorus and total hydroxide as:

$$(Ca_T) = (Ca^{2+}) + (CaPO_4^-) + (CaHPO_4) + (CaH_2PO_4^+) + (CaOH)^+ \quad (29)$$

$$(P_T) = (H_3PO_4) + (H_2PO_4^-) + (HPO_4^{2-}) + (PO_4^{3-}) + (CaPO_4^-) + (CaHPO_4) + (CaH_2PO_4^+) \quad (30)$$

$$(OH_T^-) = (OH^-) + (CaOH^+) \quad (31)$$

Then, the model (17)-(28) can be rewritten in terms of the total amounts of components as:

$$\frac{dV}{dt} = q_{in_1} + q_{in_2} - q_{out} \quad (32)$$

$$\frac{d(Ca_T)}{dt} = \frac{q_{in_1}}{V}(Ca_{Tin}) - \frac{q_{in_1}+q_{in_2}}{V}(Ca_T) - 5r_s \quad (33)$$

$$\frac{d(P_T)}{dt} = \frac{q_{in_2}}{V}(P_{Tin}) - \frac{q_{in_1}+q_{in_2}}{V}(P_T) - 3r_s \quad (34)$$

$$\frac{d(OH_T^-)}{dt} = \frac{q_{in_1}}{V}(OH_{Tin_1}^-) + \frac{q_{in_2}}{V}(OH_{Tin_2}^-) - \frac{q_{in_1}+q_{in_2}}{V}(OH_T^-) - r_s \quad (35)$$

$$\frac{d(Cl^-)}{dt} = \frac{q_{in_2}}{V}(Cl_{in}^-) - \frac{q_{in_1}+q_{in_2}}{V}(Cl^-) \quad (36)$$

Table 1. Chemical equilibria and equilibrium constants

$\{H^+\}\{H_2PO_4^-\} = K_{P_1}\{H_3PO_4\}$	(37)	$K_{P_1} = 10^{-2.147}$
$\{H^+\}\{HPO_4^{2-}\} = K_{P_2}\{H_2PO_4^-\}$	(38)	$K_{P_2} = 10^{-7.207}$
$\{H^+\}\{PO_4^{3-}\} = K_{P_3}\{HPO_4^{2-}\}$	(39)	$K_{P_3} = 10^{-12.346}$
$\{Ca^{2+}\}\{PO_4^{3-}\} = K_{Ca_1}\{CaPO_4^-\}$	(40)	$K_{Ca_1} = 10^{-6.459}$
$\{Ca^{2+}\}\{HPO_4^{2-}\} = K_{Ca_2}\{CaHPO4\}$	(41)	$K_{Ca_2} = 10^{-2.739}$
$\{Ca^{2+}\}\{H_2PO_4^-\} = K_{Ca_3}\{CaH_2PO_4^+\}$	(42)	$K_{Ca_3} = 10^{-1.407}$
$\{Ca^{2+}\}\{OH^-\} = K_{Ca_4}\{CaOH^+\}$	(43)	$K_{Ca_4} = 10^{-1.4}$
$\{H^+\}\{OH^-\} = K_W$	(44)	$K_W = 10^{-13.998}$

Additionally, the electroneutrality condition (6) holds in the liquid phase and the solution pH can be computed using (5).

Hence, the dynamics of the liquid phase are described by the differential equations (32)-(36) coupled with the algebraic equations (37)-(44).Note that the model equations employ both the species concentrations and the species activities related through (2)-(3).

4.2 Solid phase

For developing the model of the solid phase, several assumptions are made: (i) the crystals can be described by a single property coordinate L, which represents the characteristic length; (ii) the nucleation forms particles of a minimum size L_{min} at a nucleation rate r_N; (iii) the particles grow with a growth rate G, which is independent of the particles size; (iv) no breakage or agglomeration occurs. Under these assumptions, the number density function n evolves according to the population balance equation (Ramkrishna, 2000):

$$\frac{\partial n}{\partial t} + G\frac{\partial n}{\partial L} = -\frac{q_{in_1}+q_{in_2}}{V}n, \quad L_{min} < L < L_{max} \quad (45)$$

with the boundary condition

$$G(L_{min}, t)\, n(L_{min}, t) = r_N \quad (46)$$

The material flux from the liquid to the solid phase is given by

$$Vr_s = \frac{\rho_{HAP}}{M_{HAP}} \int_{L_{min}}^{L_{max}} f_v L^3 \frac{d}{dt}(V \cdot n)\, dL \quad (47)$$

where ρ_{HAP} is the density of HAP, M_{HAP} is the molecular weight of HAP and f_v is the volumetric shape factor of the crystals. Using (45), (46) and (32), the precipitation rate r_s becomes

$$r_s = \frac{\rho_{HAP}}{M_{HAP}} f_v \left(L_{min}^3 r_N + \int_{L_{min}}^{L_{max}} 3L^2 G n dL \right) \quad (48)$$

For completing the model one needs mathematical expressions and parameter values for the nucleation and growth rates. Both

of them depend highly on the degree of supersaturation, which is computed as

$$S = \left(\frac{\{Ca^{2+}\}^5 \{PO_4^{3-}\}^3 \{OH^-\}}{K_{sp}} \right)^{\frac{1}{9}} \quad (49)$$

Here we assume that the nucleation rate is given by

$$r_N = \begin{cases} R_{max} \exp\left(-\dfrac{A}{(\ln(S))^2} \right) & \text{if } S > 1 \\ 0 & \text{if } S \leq 1 \end{cases} \quad (50)$$

while the growth rate is given by

$$G = \begin{cases} k_G (S-1)^g & \text{if } S > 1 \\ 0 & \text{if } S \leq 1 \end{cases} \quad (51)$$

5. MODEL SIMULATION

The numerical values of the parameters employed in the model simulations are given in Table 2.

Table 2. Parameter values

Symbol	Value	Units	Symbol	Value	Units
ρ_{HAP}	3156	kg m^{-3}	R_{max}	3.75e11	mol m^3 s^{-1}
M_{HAP}	0.50231	kg mol^{-1}	A	40	-
f_v	0.5236	-	k_G	0.2e-5	-
			g	1.25	-

The model is implemented in Matlab as a system of differential-algebraic equations. The discretization in space of the population balance equation is done using an upwind scheme implemented in the MatMOL toolbox (Vande Wouwer et al., 2005). A grid with 1000 equidistant points has been employed in the simulations. The model has been simulated in continuous mode starting from the arbitrary initial condition $Ca_T = 4.725 \cdot 10^{-3}$mol m^{-3}, $P_T = 1.525 \cdot 10^{-3}$mol m^{-3}, $OH_T^- = 1.182 \cdot 10^{-3}$mol m^{-3}, $Cl^- = 9.677 \cdot 10^{-3}$mol m^{-3}. Constant inputs have been applied, with the following characteristics: $q_{in_1} = 0.1$m^3 s^{-1}, $(Ca_{Tin}) = 2.68 \cdot 10^{-3}$mol m^{-3}, $(OH_{Tin_1}^-) = 1.16 \cdot 10^{-2}$mol m^{-3}, $q_{in_2} = 0.5$m^3 s^{-1}, $P_{Tin} = 1.6 \cdot 10^{-3}$mol m^{-3}, $(OH_{Tin_2}^-) = 1.07 \cdot 10^{-10}$mol m^{-3}, $(Cl_{in}^-) = 4.8 \cdot 10^{-3}$mol m^{-3}. Figure 2 shows the evolutions in time of the particle size distribution, concentration of components and solution pH. The first two graphs illustrate the particle size distribution for different time instants of the experiment. At the start of the experiment ($t = 0$) no particle is present in the reactor. As expected, at low time instants a high number of small particles are formed, which indicates that nucleation is predominant. As time increases the number of particles decreases but their size increases: for example at time instant $t = 9$ the size of the crystals present in the reactor ranges from approximately $1.5 \cdot 10^{-5}$ to $3 \cdot 10^{-5}$, while at time instant $t = 10$ the size ranges from $2 \cdot 10^{-5}$ to $3.5 \cdot 10^{-5}$. At the end of the experiment a nicely centered particle size distribution is obtained: all crystals have the size in the interval $[3 \cdot 10^{-5},\ 4 \cdot 10^{-5}]$ with more crystals of size $3.5 \cdot 10^{-5}$. However, for the selected inputs an important amount of phosphate is lost via the effluent, which indicates that growing crystals of significant size while recovering high amounts of phosphorus from the effluent is not a trivial task. This motivates the need of a thorough study of the system in view of its optimal operation.

A global validation of the model is not possible since no other dynamical model for HAP crystallization under the same conditions has been proposed so far. Therefore, we present in Table 3 the validation of the thermodynamics included in the proposed model against the results provided by PHREEQC, which is one of the widely employed software for aqueous geochemical calculations. For two data points of the simulation results presented in Figure 2, characterized by certain concentration of components (Ca_T, P_T, Cl^-) and pH value, Table 3 shows the concentrations of all species respectively predicted by the model (32)-(36), (37)-(44), (45)-(46) and calculated by PHREEQC. A good correspondence between the predicted and the calculated species concentrations exists, which indicates that the model is able to accurately predict the process thermodynamics.

Table 3. Species concentrations computed by the model and by PHREEQC

Species	$Ca_T = 3.977e-04$ $P_T = 1.567e-09$ $Cl^- = 7.118e-03$ $pH = 10.9835$		$Ca_T = 3.5756e-06$ $P_T = 1.0615e-03$ $Cl^- = 4.015e-03$ $pH = 11.2361$	
	Model	PHREEQC	Model	PHREEQC
Ca^{2+}	3.9006e-04	3.900e-04	2.9172e-08	2.827e-08
$CaPO_4^-$	1.5043e-09	1.506e-09	3.5373e-06	3.539e-06
$CaHPO_4$	6.1803e-12	6.141e-12	8.1640e-09	8.041e-09
$CaH_2PO_4^+$	5.2305e-17	5.150e-17	3.9055e-14	3.782e-14
$CaOH^+$	7.5120e-06	7.650e-06	9.8776e-10	9.834e-10
H_3PO_4	9.6557e-24	9.316e-24	5.4831e-17	5.320e-17
$H_2PO_4^-$	7.0812e-15	6.884e-15	7.1580e-08	7.055e-08
HPO_4^{2-}	5.2515e-11	5.131e-11	9.5081e-04	9.495e-04
PO_4^{3-}	3.2832e-12	3.214e-12	1.0714e-04	1.081e-04
OH^-	1.0335e-03	1.043e-03	1.84e-03	1.872e-03
H^+	1.1286e-11	1.112e-11	6.3793e-12	6.230e-12

6. CONCLUSION

A novel dynamical model has been developed for the calcium phosphate crystallization under the form of hydroxyapatite. The model is based on first principles, characterizing both the solution thermodynamics and the particle size distribution. The validation of the thermodynamics with PHREEQC is presented. The model will be further used for understanding and optimally controlling the crystallization process.

ACKNOWLEDGEMENTS

The authors gratefully acknowledge the support of the WB-Green program and the research project VALMIN. This paper presents research results of the Belgian Network DYSCO (Dynamical Systems, Control, and Optimization), funded by the Interuniversity Attraction Poles Programme, initiated by the Belgian State, Science Policy Office. The scientific responsibility rests with its authors.

REFERENCES

Barone, J. and Nancollas, G. (1977). The seeded growth of calcium phosphates. the effect of solid/solution ratio in controlling the nature of the growth phase. *Journal of Colloid and Interface Science*, 62, 421–431.

Barone, J., Nancollas, G., and Tomson, M. (1976). The seeded growth of calcium phosphates. the kinetics of growth of dicalcium phosphate dihydrate on hydroxyapatite. *Calcified tissue research*, 21, 171–182.

Boistelle, R. and Astier, J. (1988). Crystallization mechanisms in solution. *Journal of Crystal Growth*, 90, 14–30.

Boistelle, R. and Lopez-Valero, I. (1990). Growth units and nucleation: the case of calcium phosphates. *Journal of Crystal Growth*, 102, 609–617.

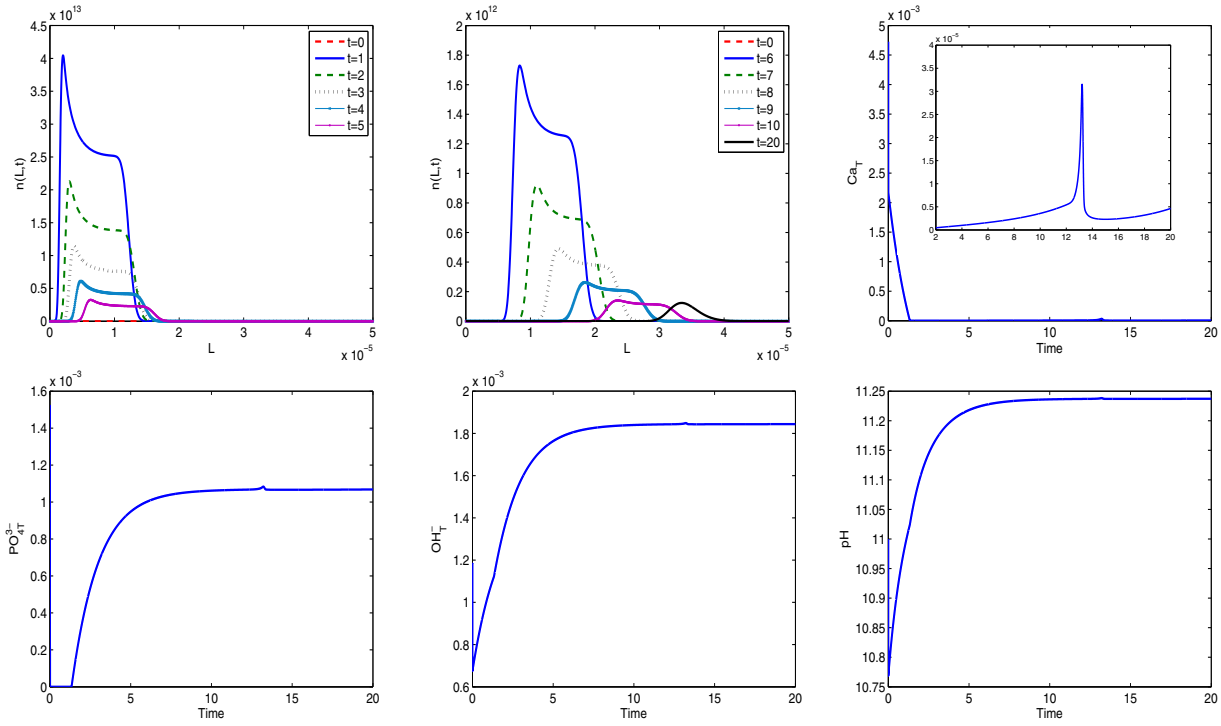

Fig. 2. Model simulation in a continuous operation for constant inputs: $q_{in_1} = 0.1\text{m}^3\ \text{s}^{-1}$, $q_{in_2} = 0.5\text{m}^3\ \text{s}^{-1}$

Castro, F., Ferreira, A., Rocha, F., Vicente, A., and Teixeira, J. (2012). Characterization of intermediate stages in the precipitation of hydroxyapatite at 37°c. *Chemical Engineering Science*, 77, 150–156.

Castro, F., Kuhn, S., Jensen, K., Ferreira, A., Rocha, F., Vicente, A., and Teixeira, J. (2013). Process intensification and optimization for hydroxyapatite nanoparticles production. *Chemical Engineering Science*, 100, 352–359.

Fernandez, E., Gil, F., Ginebra, M., Driessens, F., Planell, J., and Best, S. (1999a). Calcium phosphate bone cements for clinical applications part i: Solution chemistry. *Journal of Materials Science: Materials in Medicine*, 10, 169–176.

Fernandez, E., Gil, F., Ginebra, M., Driessens, F., Planell, J., and Best, S. (1999b). Calcium phosphate bone cements for clinical applications part ii: Precipitate formation during setting reactions. *Journal of Materials Science: Materials in Medicine*, 10, 177–183.

Galbraith, S. and Schneider, P. (2014). Modelling and simulation of inorganic precipitation with nucleation, crystal growth and aggregation: A new approach to an old method. *Chemical Engineering Journal*, 240, 124–132.

Hanhoun, M., Montastruc, L., Azzaro-Pantel, C., Biscans, B., Frèche, M., and Pibouleau, L. (2013). Simultaneous determination of nucleation and crystal growth kinetics of struvite using a thermodynamic modeling approach. *Chemical Engineering Journal*, 215-216, 903–912.

Hosni, K., Ben Moussa, S., Chachi, A., and Ben Amor, M. (2008). The removal of po_4^{3-} by calcium hydroxide from synthetic wastewater: optimisation of the operating conditions. *Desalination*, 223, 337–343.

Jiang, K., Zhou., K., Yang, Y., and Du, H. (2014). Growth kinetics of calcium fluoride at high supersaturation in a fluidized bed reactor. *Environmental Technology*, 35, 81–88.

Jones, A. (2002). *Crystallization Process Systems*.

Koutsoukos, P., Amjad, Z., Tomson, M., and Nancollas, G. (1980). Crystallization of calcium phosphates. a constant composition study. *Journal of the American Chemical Society*, 102, 1553–1557.

Mullin, J. (2001). *Crystallization*. Butterworth-Heinemann, Oxford.

Nancollas, G. and Gardner, G. (1974). Kinetics of crystal growth of calcium oxalate monohydrate. *Journal of Crystal Growth*, 21, 267276.

Nancollas, G. and Koutsoukos, P. (1980). Calcium phosphate nucleation and growth in solution. *Crystal Growth Charact.*, 3, 77–102.

Oliveira, C., Georgieva, P., Rocha, F., and Feyo de Azevedo, A.F.S. (2007). Dynamical model of brushite precipitation. *Journal of Crystal Growth*, 305, 201–210.

Parkhurst, D. and Appelo, C. (2013). *Description of input and examples for PHREEQC version 3A computer program for speciation, batch-reaction, one-dimensional transport, and inverse geochemical calculations: U.S. Geological Survey Techniques and Methods*.

Ramkrishna, D. (2000). *Population Balances. Theory and Applications to Particulate Systems in Engineering*. Academic Press, New York.

Söhnel, O. and Garside, J. (1992). *Precipitation*. Butterworth-Heinemann, Oxford.

Song, Y., Hahn, H., and Hoffmann, E. (2002). Effects of solution conditions on the precipitation of phosphate for recovery. a thermodynamic evaluation. *Chemosphere*, 48, 1029–1034.

Vande Wouwer, A., Saucez, P., Schiesser, W., and Thompson, S. (2005). A matlab implementation of upwind finite differences and adaptive grids in the method of lines. *Journal of Computational and Applied Mathematics*, 183, 245–258.

Vedantam, S. and Ranade, V. (2013). Crystallization: Key thermodynamic, kinetic and hydrodynamic aspects. *Sadhana*, 38, 1287–1337.

Wang, L. and Nancollas, G. (2008). Calcium orthophosphates: Crystallization and dissolution. *Chemical Reviews*, 108, 4628–4669.